either a change in alkyne substituents or metal fragments has much influence on the perturbation of the alkyne. This structure analysis also confirms that the metal–metal bond bridged perpendicularly by the acetylene (Fe(1)–Fe(3) = 2.5666 (5) Å) is quite significantly longer than either of the other Fe–Fe bonds (Fe(1)–Fe(2) = 2.4734 (5), Fe(2)–Fe(3) = 2.4749 (5) Å).

A theoretical model[13] for the cleavage of the alkyne triple bond in the related trirhodium cluster $Cp_3Rh_3(CO)(\mu_3\text{-}\eta^2\text{-}\parallel\text{-}PhC_2Ph)$ to generate a bis(alkyidyne) species suggests that rotation of the acetylene from a $\mu_3\text{-}\eta^2\text{-}\parallel$- to a $\mu_3\text{-}\eta^2\text{-}\perp$-position occurs, followed by edge coordination of the alkyne, CO loss, and alkylidyne formation. It is interesting to compare this postulate with the structure of the present complex since the $C(13)\text{–}C_2H_5$ group is already "alkylidyne-like" structurally and C(12) is much more "edge coordinated". Figure 2 shows however that scission of the C(12)–C(13) bond and rotation of the $C(12)\text{–}C_2H_5$ group around the Fe(1)–Fe(3) bond to bridge the bottom face of the cluster might be impaired by steric interactions between the substituent ethyl group on C(12) and the equatorial carbonyls of the $Fe(CO)_3$ units unless significant Fe(1)–Fe(3) bond lengthening and/or reorientation of the alkyl groups to slide between the equatorial CO's occurred in the transition state. On the other hand, such a rotation leading to skeletal isomerism might be more favorable with an alkyne bearing hydrogen or a smaller group than Et on C(12). CNDO calculations on $Fe_3(CO)_9(\mu_3\text{-}\eta^2\text{-}\perp\text{-}EtC_2H)]$ suggest that the site C_α [C(13) in $Fe_3(CO)_9(\mu_3\text{-}\eta^2\text{-}\perp\text{-}EtC_2Et)$] should be positively charged and hence favored by electron-releasing substituents. Keeping this in mind a particularly favorable situation for conversion of $Fe_3(CO)_9(\mu_3\text{-}\eta^2\text{-}\perp\text{-}RC_2R')$ to $Fe_3(CO)_9(\mu_3\text{-}CR)(\mu_3\text{-}CR')$ might be found for monosubstituted alkynes with an electron-releasing substituent at C_α and unsubstituted at C_β. Interestingly, Shriver[10] has recently prepared an unstable complex of this type in solution and found a smooth conversion to a bis(alkylidyne) cluster at room temperature.

Acknowledgment. We are grateful to the Natural Sciences and Engineering Research Council of Canada for financial support of this work.

Registry No. $Fe_3(CO)_9(\mu_3\text{-}\eta^2\text{-}\perp\text{-}C_2Et_2)$, 69402-19-3; $Fe_3(CO)_{12}$, 17685-52-8; Fe, 7439-89-6.

Supplementary Material Available: A table of anisotropic thermal parameters (Table S1) (1 page); a listing of structure factors (Table S2) (15 pages). Ordering information is given in any current masthead page.

Sterically Hindered Aryloxide-Substituted Alkylaluminum Compounds

Andrew P. Shreve,† Rolf Mulhaupt,† William Fultz,† Joseph Calabrese, Wayne Robbins, and Steven D. Ittel*

Central Research & Development Department,‡ E. I. du Pont de Nemours & Company, Wilmington Delaware 19898

Received June 25, 1987

Aluminum alkyl reagents react with sterically hindered phenols such as 2,6-di-*tert*-butyl-4-methylphenol (BHT) to liberate alkane and generate alkylaluminum phenoxides. This substitution chemistry has been followed by NMR techniques, and the products of the reactions have been characterized by NMR and by X-ray crystallography. In the reaction with trimethylaluminum, observed species are Al_2Me_6, Al_2Me_5BHT, $AlMe_2BHT$, and $AlMeBHT_2$. At intermediate stages of reaction, all four species are observed in dynamic equilibrium. In the $AlEt_3$ system, the corresponding Al_2Et_5BHT is not observed. In the $Al(i\text{-}Bu)_3$ system, the two monomeric products are formed sequentially. The alkylaluminum phenoxides react with Lewis bases to form four-coordinate molecules of relevance to Ziegler–Natta catalysts that display both high activity and high stereospecificity. The compound $AlMeBHT_2$ crystallizes in the triclinic space group $P\bar{1}$ with unit-cell dimensions a = 12.108 (2) Å, b = 12.793 (2) Å, c = 10.981 (1) Å, α = 102.65 (1)°, β = 110.54 (1)°, and γ = 68.16 (1)°. The methyl toluate adduct $AlEt_2BHT(MeC_6H_4CO_2Me)$ crystallizes in the monoclinic space group $C2/c$ with unit-cell dimensions a = 24.554 (4) Å, b = 14.924 (2) Å, c = 15.216 (2) Å, and β = 91.01 (1)°.

Introduction

The early work of Jeffery and Mole[1] demonstrated that aluminum alkyl reagents could be modified readily by reaction with phenols. This approach has been the subject of considerable subsequent work in a number of laboratories.[2-4] While simple phenols give compounds that are bridged through the oxygen atoms of the resulting phenoxide group, sterically hindered phenols give products that are monomeric in nature. These monomeric species, usually synthesized from 2,6-di-*tert*-butyl-substituted phenols, have found application in organic synthesis[5,6] and

†Current addresses: A.P.S., Department of Chemistry, Cornell University, Ithaca, NY; R.M., Ciba Geigy AG, Forschungszentrum KA/Marly, CH-1701 Fribourg, Switzerland; W.F., J. M. Huber Corp., P.O. Box 310, Havre de Grace, MD 21078.

‡Contribution No. 4414.

(1) Jeffrey, E. A.; Mole, T. *Aust. J. Chem.* **1968**, *21*, 2683.

(2) (a) Pasynkiewicz, S.; Starowieyski, K. B.; Skowronska-Ptasinska, M. *J. Organomet. Chem.* **1973**, *52*, 269. (b) Starowieyski, K. B.; Pasynkiewicz, S.; Skowronska-Ptasinska, M. *J. Organomet. Chem.* **1974**, *65*, 155. (c) Starowieyski, K. B.; Pasynkiewicz, S.; Skowronska-Ptasinska, M. *J. Organomet. Chem.* **1975**, *90*, C43–44. (d) Pasynkiewicz, S.; Starowieyski, K. B.; Peregudov, A. S.; Kravtsov, D. N. *J. Organomet. Chem.* **1977**, *132*, 191. (e) Skowronska-Ptasinska, M.; Starowieyski, K. B.; Pasynkiewicz, S. *J. Organomet. Chem.* **1977**, *141*, 149. (f) Starowieyski, K. B.; Skowronska-Ptasinska, M.; Muszynski, J. *J. Organomet. Chem.* **1978**, *157*, 379. (g) Skowronska-Ptasinska, M.; Starowieyski, K. B.; Pasynkiewicz, S.; Carewska, M. *J. Organomet. Chem.* **1978**, *160*, 403.

(3) Panasenko, A. A.; Khalilov, L. M.; Kuchin, A. V.; Tolstikov, G. A. *Izv. Akad. Nauk SSSR, Ser. Khim.* **1980**, 2652.

(4) Yoon, N. M.; Gyoung, Y. S. *J. Org. Chem.* **1985**, *50*, 2443.

0276-7333/88/2307-0409$01.50/0

Table I. Proton NMR Spectra (in ppm) of Aluminum Compounds

	temp,	alkyl			phenoxide		
	°C	α-CH	β-CH	γ-CH	*t*-Bu	4-Me	3,5-H
Al_2Me_6	25	−0.29					
	−80	0.33[b]					
		−0.55[c]					
Al_2Me_5B/ $AlMe_2B$	−80	−0.21			1.41	2.07	7.07
$AlMeB_2$	25	−0.23			1.61	2.35	7.13
	−80	0.11			1.58	2.36	7.21
Al_2Et_6	25	0.29	1.08				
	−80	0.63	0.91[b]				
		0.09	1.22[c]				
$AlEt_2B$	25	0.23	1.09		1.45	2.26	7.06
	−80	0.19	1.15		1.44	2.31	7.09
$AlEtB_2$	25	0.39	0.87		1.59	2.29	7.15
	−80	0.48	0.87		1.59	2.34	7.19
Al-*i*-Bu_3	25	0.25	1.91	0.98			
	−80	0.32	1.96	1.10			
Al-*i*-Bu_2B	25	0.37	1.94	0.98	1.41	2.19	6.96
	−80	0.32	2.01	1.06	1.46	2.31	7.10
Al-*i*-BuB_2	25	0.39	1.7	0.71	1.53	2.21	7.03
	−80	0.34	*a*	0.74	1.60	2.31	7.17

[a] Not observed. [b] Bridging. [c] Terminal.

the preparation of a new generation of Ziegler–Natta catalysts that display the unusual combination of high activity and high stereospecificity in the polymerization of propene.[7-14] (Throughout this paper 2,6-di-*tert*-butyl-4-methylphenol is referred to as H-BHT from the trivial name, butylated hydroxytoluene. The resulting phenoxide is referred to as BHT.) We have recently reported the application of vapor synthesis to the preparation of magnesium chloride supported Ziegler–Natta catalysts.[15] In normal catalyst systems, there are a wide variety of stereospecific and nonstereospecific, catalytically active centers producing isotactic and atactic polypropylene, respectively. Addition of Lewis base electron donors poisons the more acidic, nonstereospecific sites to a greater extent than the stereospecific sites, thereby increasing the proportion of the desired isotactic polypropylene.[16] The vapor-synthesized catalysts, and later

Table II. Thermodynamics of the $AlEt_xBHT_{3-x}$ System

$2AlEt_2BHT \rightleftharpoons \frac{1}{2}(AlEt_3)_2 + AlEtBHT_2$

temp, °C	K_{eq}	ΔG, kcal
27	0.010	2.74
0	0.019	2.14
−30	0.038	1.57
−60	0.061	1.18
−80	0.137	0.76

[a] $\Delta H^{\ddagger} = -2.83$ kcal/mol; $\Delta S^{\ddagger} = -18.6$ eu.

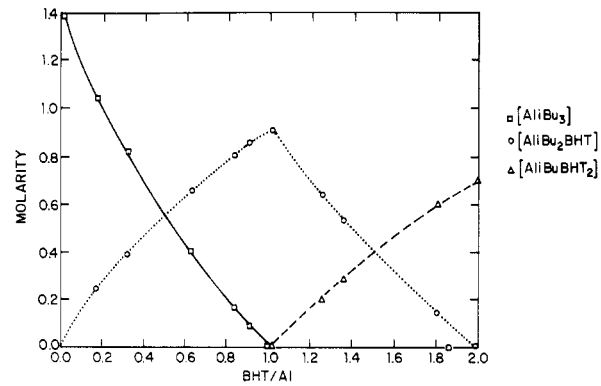

Figure 1. Composition of the $Al(i\text{-}Bu)_xBHT_{3-x}$ system as a function of BHT to aluminum ratio.

conventionally prepared catalysts based upon the insights gained from the vapor-synthesized systems, display nonclassical behavior—stereoselectivity and activity increase simultaneously as small portions of ethyl toluate are added as a Lewis base.[17] As the proportion of Lewis base is increased further, the activity ceases to increase and then begins to decrease in a more classical type of behavior. The essential, differentiating feature of these catalysts is the incorporation of sterically hindered phenols into both the catalyst preparation and catalyst activator. To better understand the basis for this nonclassical behavior, we have initiated a program on the chemistry of hindered phenols in Ziegler–Natta related systems.

Experimental Section

General Data. All solvents were purified and dried by standard techniques.[18] Aluminum alkyls were used as received from Texas Alkyls. H-BHT from Aldrich was recrystallized from pentane; methyl benzoate was used as received. All glassware used in synthetic work was either flame- or oven-dried. NMR spectra were recorded on NT series GE spectrometers at 300- or 360-MHz proton frequencies and are presented in Table I. Chemical shifts were referenced to residual protic solvent peaks or internal TMS. Spectra were recorded in standard pulsed FT mode at constant temperature which was calibrated by using a precalibrated thermocouple. Infrared spectra were recorded on a Perkin-Elmer Model 983G optical null spectrophotometer using an o-ring sealed IR cell and standard salt plates. Spectra were either run as neat liquid samples or as Nujol mulls as appropriate. Elemental analyses and vapor pressure osmometry molecular weight determinations were performed by Galbraith Laboratories, Knoxville, TN.

Reactions of Aluminum Alkyls with BHT. Stock solutions of BHT (2.8 M) and the appropriate aluminum alkyls (1.4 M) were prepared in carefully dried septum vials. Appropriate volumes of the two solutions were syringed into new vials and

(5) (a) Iguchi, S.; Nakai, H.; Hayashi, M.; Yamamoto, H. *J. Org. Chem.* **1979**, *44*, 1363. (b) Itoh, A.; Oshima, K.; Yamamoto, H.; Nozaki, H. *Bull. Chem. Soc. Jpn.* **1980**, *53*, 2050. (c) Iguchi, S.; Nakai, H.; Hayashi, M.; Yamamoto, H.; Maruoka, K. *Bull. Chem. Soc. Jpn.* **1981**, *54*, 3033. (d) Sakane, S.; Fukiwara, J.; Maruoka, K.; Yamamoto, H. *J. Am. Chem. Soc.* **1983**, *105*, 6154. (e) Maruoka, K.; Itoh, T.; Yamamoto, H. *J. Am. Chem. Soc.* **1985**, *107*, 4573.

(6) Giannini, U.; Albizzati, E.; Parodi, S. Ger. Offen. DE 2630585, 1977 (Montedison S.p.A.).

(7) Giannini, U.; Albizzati, E.; Parodi, S. Ger. Offen. DE 2630585, 1977, (Montedison S.p.A.).

(8) (a) Langer, A. W., Jr. Eur. Pat. Appl. EP 15762, 1980, (Exxon Res. and Eng. Co.). (b) Langer, A. W. US 4377720 A, 1983 (Exxon Res. and Eng. Co.). (c) Langer, A. W. US 4304684 A, 1981 (Exxon Res. and Eng. Co.). (d) Langer, A. W., Jr. US 4410750 A, 1983, (Exxon Res. and Eng. Co.). (e) Langer, A. W., Jr. US 4434313 A, 1984, (Exxon Res. and Eng. Co.).

(9) Band, E. I.; Breen, M. J. Eur. Pat. Appl. EP 164789 A2 1985, (Stauffer Chemical Co.).

(10) Goodall, B. L. In *Transition Metal Catalyzed Polymerizations*; Quirk, R. P., Ed.; Harwood Academic: New York, 1983; p 355.

(11) Keii, T.; Soga, K., Eds. *Catalytic Polymerization of Olefins*; Elsevier: New York, 1986.

(12) Goodall, B. L. *J. Chem. Educ.* **1986**, *63*, 191.

(13) Mulhaupt, R.; Klabunde, U.; Ittel, S. D. *J. Chem. Soc., Chem. Commun.* **1985**, 1745.

(14) Ittel, S. D.; Mulhaupt, R.; Shreve, A. P.; Klabunde, U. In *Homogeneous and Heterogeneous Catalysis*; Yermakov, Y., Likholobov V., Eds.; VNU Press: Utrecht, 1986; p 431.

(15) (a) Ittel, S. D.; Mulhaupt, R.; Klabunde, U. *J. Polym. Sci., Polym. Chem.* **1986**, *24*, 3447. (b) Klabunde, U.; Mulhaupt, R. U. S. Patent 4650778, 1987.

(16) (a) Chien, J. C. W.; Wu, J.-C. *J. Polym. Sci., Polym. Chem.* **1982**, *20*, 2445. (b) Busico, V.; Corradini, P.; De Martino, L.; Proto, A.; Savino, V. *Makromol. Chem.* **1985**, *186*, 1279.

(17) Mulhaupt, R.; Ovenall, D. W.; Ittel, S. D. *J. Polym. Sci., Polym. Chem. Ed.*, submitted for publication.

(18) Shriver, D. F. *The Manipulation of Air-sensitive Compounds* McGraw-Hill: New York, 1969.

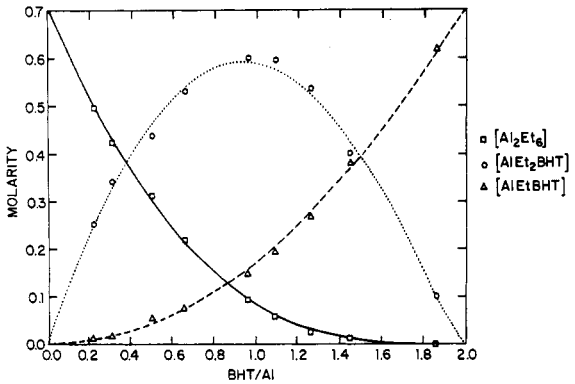

Figure 2. Composition of the $AlEt_xBHT_{3-x}$ system as a function of BHT to aluminum ratio.

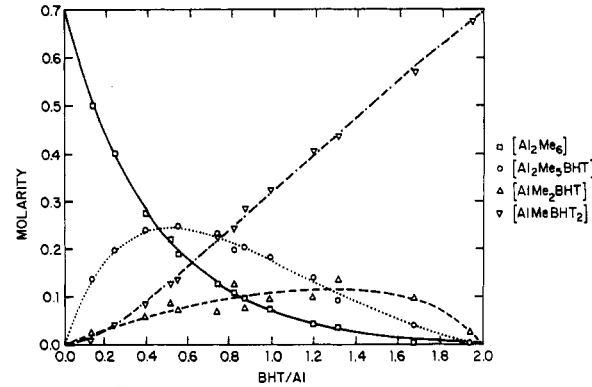

Figure 3. Composition of the $AlMe_xBHT_{3-x}$ system as a function of BHT to aluminum ratio.

allowed to react for several minutes and were stirred for several minutes after the addition was complete. Nitrogen was bubbled through the mixture by using a large syringe (20 or 50 mL) to remove dissolved gas from the solution. The sample was then transferred to an NMR tube, capped, and sealed with Parafilm. The NMR tubes were kept in the glovebox until the spectra were ready to be run. The above general procedure was found to give more consistent results than addition of neat aluminum alkyl to a H-BHT solution.

The integrated intensities from the NMR spectra were used to assign relative concentrations of the various species in solution. The relative concentrations were then used to calculate the molar concentrations of each of the observed species by using the known total molar concentration of aluminum in the solution. In the case of the trimethylaluminum reactions at −80 °C in toluene-d_8 and in pentane-d_{12} at −120 °C, the methyl groups of the two species Al_2Me_5BHT and $AlMe_2BHT$ were still in fast exchange on the NMR time scale. Their relative concentrations were determined by comparison of the ratio of the BHT *tert*-butyl resonance and the methyl resonance. At low relative BHT, their relative intensities indicated about 5:1 Me to BHT ratio, but at high relative BHT this ratio was closer to 2:1.

The raw data was put into RS/1, a data analysis system from BBN Research Systems. The data was converted to a pseudo-concentration vs time plot by treating the BHT/Al as conversion and setting:

$$t = -\ln (1 - 0.5\mathrm{BHT/Al})$$

The concentrations of the various species were fit as reactants (Al_2Me_6, Al_2Et_6, etc.), intermediates (Al_2Me_5BHT, $AlMe_2BHT$, $AlEt_2BHT$, etc.) and products ($AlMeBHT_2$, $AlEtBHT_2$, etc.) of a series of first-order reactions. The equations were fit by using the "fit function" routines within RS/1 to determine the rate constant(s).

The x axes were then changed back to BHT/Al, and the results are presented in Figures 1–3. The equilibrium constants were calculated from the rough data except for the $AlMe_5BHT$ and $AlMe_2BHT$ concentrations. Since the sum of the two could be measured accurately, but the assignment of relative ratios was difficult, a high value of Al_2Me_5BHT, for instance, gave a low value of $AlMe_2BHT$. A minor shift in estimated concentration gave a large shift in the calculated equilibrium constant. The values of Al_2Me_5BHT and $AlMe_2BHT$ were smoothed by using a three-point running average, weighted for the slight irregularities in the distribution of data points along the BHT/Al axes. The equilibrium constants for the disproportionation reactions (see eq 2, 4, and 5 in the results) were calculated as

$$\mathrm{AlMe_3–BHT\ System:}\quad K_4 = [Al_2Me_6]^{1/2}[AlMe_2B][Al_2Me_5B]^{-1}$$

$$K_4 = 0.143\ (20)$$

$$K_5 = [Al_2Me_5B][AlMeB_2][AlMe_2B]^{-3}$$

$$K_5 = 55.5\ (55)$$

$$\mathrm{AlEt_3–BHT\ System:}\quad K_2 = [Al_2Et_6]^{1/2}[AlEtB_2][AlEt_2B]^{-2}$$

$$K_2 = 0.137\ (20)$$

Reaction of $AlEt_3$ with H-BHT and Methyl Toluate. H-BHT (0.32 g, 1.4 mmol) was dissolved in benzene-d_6 (1 mL) in a sample vial. This solution was reacted with an appropriate amount of $AlEt_3$ in benzene-d_6 (1 mL). After this reaction mixture was degassed, an appropriate amount of methyl toluate dissolved in benzene-d_6 was slowly added (for reference, 0.22 g of methyl toluate is 1.4 mmol). The solution turned yellow upon addition of the ester. The mixture was allowed to stir for 15 min before an NMR sample was withdrawn. The benzene was allowed to evaporate from the remainder of the sample, and the residue was used for infrared analysis.

Reaction of $AlEtBHT_2$ with *tert*-Butyl Alcohol. $AlEtBHT_2$ (0.1 g, 0.2 mmol) was dissolved in benzene-d_6 in a sample vial. An appropriate amount of neat *tert*-butyl alcohol was added by syringe while stirring. The mixture was allowed to stir for several minutes, and then samples were withdrawn for NMR analysis.

Attempted Synthesis of $AlEt_2BHT$. H-BHT (3.2 g, 14 mmol) was dissolved in pentane (10 mL), and $AlEt_3$ (2.0 mL, 14 mmol) in pentane (20 mL) was added slowly. After the solution was stirred for an hour, the pentane was evaporated, giving a solid precipitate which was tacky to the touch. After the mixture was left standing for 48 h, there remained a white solid suspended in a thick viscous liquid. The solid was collected and identified as $AlEtBHT_2$, and the liquid was found to contain significant amounts of $AlEt_3$, $AlEtBHT_2$, and some $AlEt_2BHT$.

$AlEtBHT_2$. Method I. H-BHT (32.0 g, 0.14 mol) was dissolved in heptane to make 100 mL of solution. $AlEt_3$ (10.0 mL, 0.07 mol) was added to 50 mL of heptane. The H-BHT solution was added by cannula over a 70-min period to the $AlEt_3$ solution which was under reflux. The solution was stirred and refluxed for an additional 70 min before being allowed to cool slowly to room temperature. The heptane was removed under vacuum to leave a white solid. The product was recrystallized by dissolving in hot heptane, cooling to −35 °C, and collecting the resulting solid by filtration (24.7 g, recrystallized yield of 68%). **Method II.** An alternative and simpler synthesis involved addition of 2 equiv of H-BHT in hexane to 1 equiv of $AlEt_3$ in hexane. The resulting mixture was allowed to stir for 2 h after which time the product began to crystallize. The remaining solvent was pumped off, and the crude product was collected in good yield; mp 176–179 °C. NMR: data are presented in Table I; IR (Nujol, (cm^{-1}, % T): 1346, 47; 1281, 17; 1260, 32; 1223, 21; 1212, 22; 1118, 57; 1027, 50; 919, 49; 861, 39; 817, 44; 801, 36; 780, 45; 726, 50; 644, 55; 601, 45; 527, 39. Anal. Calcd for $C_{32}H_{51}AlO_2$: C, 77.7; H, 10.4. Found: C, 77.6; H, 10.3.

$AlMeBHT_2$. This synthesis was carried out by using method I above. The recrystallized yield was 87%. IR (Nujol, cm^{-1}, % T): 1348, 41; 1280, 18; 1261, 29; 1223, 27; 1210, 27; 1118, 46; 1026, 50; 918, 51; 860, 34; 817, 41; 800, 36; 779, 43; 727, 52; 644, 51; 600, 43; 527, 40. Anal. Calcd for $C_{31}H_{49}AlO_2$: C, 77.5; H, 10.3; mol wt (C_6H_6), 481. Found: C, 77.6; H, 10.3; mol wt (C_6H_6), 475.

Al(*i*-Bu)BHT_2. This synthesis was done as described in method I for $AlEtBHT_2$, using H-BHT (32.0 g, 0.14 mol) and $Al(i\text{-}Bu)_3$ (18.5 mL, 0.07 mol). Product (29.76 g) was collected from the first recrystallization to give a recrystallized yield of 78.1%. IR (Nujol): very similar to those above. Anal. Calcd for $C_{34}H_{55}AlO_2$: C, 78.1; H, 10.6. Found: C, 78.0; H, 10.8.

Table III. Summary of X-ray Diffraction Data

complex	$AlMeBHT_2$	$AlEt_2BHT{\cdot}MeO_2CC_6H_4Me$
formula	$AlO_2C_{31}H_{49}$	$AlO_3C_{28}H_{43}$
fw	480.71	454.63
space group	$P\bar{1}$ (No. 2)	$C2/c$ (No. 15)
a, Å	12.108 (2)	24.554 (4)
b, Å	12.793 (2)	14.924 (2)
c, Å	10.981 (1)	15.216 (2)
α, deg	102.65 (1)	90
β, deg	110.54 (1)	91.01 (1)
γ, deg	68.16 (1)	90
V, Å^3	1470.8	5574.9
Z	2	8
D(calcd), g cm^{-3}	1.085	1.086
cryst dimen, mm	0.35 × 0.30 × 0.35	0.24 × 0.17 × 0.30
temp, °C	−100	−100
radiatn	Mo Kα (0.71069 Å, graphite monochromator)	
μ, cm^{-1}	0.88	0.924
2θ limits, deg	4.2–55.0	4.0–50.0
no. of unique obsd. data, $I \geq 3\sigma(I)$	7116, 3520	5281, 1707 ($\geq 2.5\sigma$)
final no. of variables	307	289
final residual, e Å^{-3}	0.37	0.18
R	0.053	0.074
R_w	0.050	0.061

Attempted Synthesis of $AlBHT_3$. Procedure I. The synthesis was attempted by using the same general procedure as in method I of syntheses section using H-BHT (3.2 g, 14 mmol) and $AlEt_3$ (0.5 mL, 3.5 mmol). The H-BHT solution was added to the $AlEt_3$ as quickly as was permitted by the evolution of ethane. The reaction mixture was pumped to dryness. There was no evidence of formation of $AlBHT_3$ by NMR analysis. The product was found to be predominantly $AlEtBHT_2$ with a significant amount of unreacted H-BHT. **Procedure II.** H-BHT (3.2 g, 14 mmol) was melted on a hot plate in glovebox. While stirring, $AlEt_3$ (0.25 mL, 1.75 mmol) was added to the melt. The mixture was allowed to continue stirring on the hot plate after the addition was complete. After a few minutes, the mixture turned yellow, characteristic of a decomposed aluminum phenoxide. After cooling an NMR of the resulting viscous, light yellow suspension gave no evidence of $AlBHT_3$. The major component was free H-BHT, and there were complex NMR signals, evidently from decomposed phenoxide products.

$AlEt_2BHT$(MT). $AlEt_3$ (4.1 mL, 0.03 mol) was added to 40 mL of pentane. To this solution was added, slowly by syringe, a solution of H-BHT (6.6 g, 0.03 mol) in 20 mL of pentane. The resulting solution was stirred for 20 min, and then methyl toluate (4.5 g, 0.03 mol) dissolved in pentane was added slowly. The resulting complexation reaction was quite exothermic, bringing the pentane to reflux. The mixture was allowed to stir for $1^1/_2$ hours, after which time a large amount of yellow solid had precipitated. The pentane supernatant was decanted, and the remaining solid was washed with three 15-mL portions of pentane. The resulting yellow solid was pumped to complete dryness and collected to give 8.0 g of solid product. A portion of crude product was recrystallized by dissolving in hot toluene and cooling the resulting solution to −25 °C; mp 127–128 °C. IR (Nujol, cm^{-1}, % T); 1657, 40; 1635, 12; 1604, 37; 1335, 21; 1301, 10; 1223, 37; 1203, 37; 1158, 46; 1135, 40; 1078, 60; 1026, 55; 1003, 65; 918, 65; 864, 48; 800, 36; 779, 43; 725, 32; 644, 51. Anal. Calcd for $C_{28}H_{43}AlO_3$: C, 74.0; H, 9.53. Found: C, 74.1; H, 9.6.

X-ray Structure Determinations. Many of the details of the two crystal structures are given in Table III. The crystals were mounted and sealed in capillaries under nitrogen. Lattice constants were verified by partial rotation photographs along each crystallographic axis.

$AlMeBHT_2$ Structure. Data was collected on a Syntex R3 diffractometer using the ω-scan method. The scan width of 1.50° ω was done at scan speeds of 2.00–9.80°/min, and a typical half-height peak width was 0.43° ω. The three standards, which were collected 37 times, showed a 3% fluctuation. The minimal variation in azimuthal scans together with the small absorption coefficients obviated the need for absorption correction. The structure was solved by direct methods (MULTAN)[19] after the input of a model to bias the correct phase solution. The solution had the second best figure of merit of 32 possible solutions. Refinement was carried out by full-matrix least squares on F, using scattering factors from the *International Tables for X-ray Crystallography*, Kynoch Press, Birmingham, England, 1974, Vol. IV, and including the anomalous terms for aluminum. All nonhydrogen atoms were refined anisotropically. The hydrogen atom positions were fixed. Several reflections were inconsistent as indicated by a biweight analysis and were seen to have electronic spikes due to diffractometer problems. The largest residual density of 0.37 e/Å^3 was near carbon atom 23.

$AlEt_2BHT(MeO_2CC_6H_4Me)$ Structure. Data was collected on a Syntex P3 diffractometer using the ω scan method. The scan width of 1.40° ω was done at scan speeds of 4.00–10.00°/min, and the ratio of background counting to scan time was 1.0. The three standards, which were collected every 200 reflections, showed a 2.5% fluctuation. Lorentz and polarization corrections were applied, but an absorption correction was not required. The crystal was a weak diffractor, so the number of observed reflections was low. The structure as solved by direct methods (MULTAN). Refinement was carried out by full-matrix least squares of F, using scattering factors from the *International Tables for X-ray Crystallography*, Kynoch Press, Birmingham, England, 1974, Vol. IV, and including the anomalous terms for aluminum. All nonhydrogen atoms were refined anisotropically. The hydrogen atom positions were calculated. In a final difference map, the largest residual density of 0.18 e/Å^3 was 1.80 Å from the aluminum atom.

Results

NMR Studies. The phenolic functionality of butylated hydroxytoluenes (H-BHT) reacts rapidly with aluminum alkyls, liberating alkanes and giving sterically hindered aluminum phenoxides according to the general reaction shown in (1). Of the three aluminum alkyls used in this

$$AlR_3 \xrightarrow[-RH]{\text{H-BHT}} R_2AlBHT \xrightarrow[-RH]{\text{H-BHT}} RAlBHT_2 \xrightarrow[-RH]{\text{H-BHT}} AlBHT_3 \quad (1)$$

study, Al(i-Bu)$_3$ shows the simplest behavior. Monomeric Al(i-Bu)$_3$ reacts completely with the first equivalent of added H-BHT to give 1 equiv of Al(i-Bu)$_2$BHT. As the second equivalent of H-BHT is added, the initial product is consumed and Al(i-Bu)BHT_2 is formed. Continued addition of H-BHT beyond 2 equiv produces no further reaction, and resonances attributable to free H-BHT grow into the NMR spectra. This behavior is depicted in Figure 1. The compound Al(i-Bu)$_2$BHT has been reported to be a stable,[2g] monomeric liquid at room temperature. It can be induced to undergo disproportionation to Al(i-Bu)$_3$ and Al(i-Bu)BHT_2 at 110 °C and 10^{-4} Torr; under these conditions, the liberated Al(i-Bu)$_3$ is removed as a vapor, driving the reaction to completion.

The reaction of the H-BHT with Al_2Et_6 gives the same general pattern of behavior but is complicated by the dimeric nature of the starting material. There is also a complicating equilibrium whereby the mono(phenoxide) disproportionates to bis(phenoxide) and starting aluminum alkyl. Again, the initial species formed is $AlEt_2BHT$, but even at very early stages of addition, $AlEtBHT_2$ is observed. The three species Al_2Et_6, $AlEt_2BHT$, and $AlEtBHT_2$ are all observed simultaneously in a dynamic equilibrium. At room temperature, the ethyl groups of Al_2Et_6 and $AlEt_2BHT$ are in fast exchange on the NMR time scale, but the resonances of $AlEtBHT_2$ are distinct. As the temperature is lowered to −80 °C, the exchange process is slowed and resonances attributable to the ter-

(19) The crystallographic software was written by J. C. Calabrese and includes MULTAN78 (Main, P.; Lessinger, L.; Woolfson, M. M.; Germain, G.; Declerq, J. P.; York, England, and Louvain-la-Neuve, Belgium, 1978) and ORTEP (C. K. Johnson, Oak Ridge, TN, 1976).

minal and bridging alkyl groups of Al_2Et_6, $AlEt_2BHT$, and $AlEtBHT_2$ are observed. It is also observed that as the temperature is lowered, the relative concentrations of Al_2Et_6 and $AlEtBHT_2$ increase at the expense of $AlEt_2BHT$. The reversible equilibrium established by disproportionation of $AlEt_2BHT$ can be expressed by eq 2. A quantitative study of this system yields the data

$$2AlEt_2BHT \overset{K_2}{\rightleftharpoons} {}^1/_2Al_2Et_6 + AlEtBHT_2 \quad (2)$$

displayed in Figure 2 together with calculated curves derived from a model of the system. The equilibrium constant, K_2, is 0.137 $M^{-1/2}$ at −80 °C.

It had been reported earlier[2g] that in the sequential reaction of H-BHT with Al_2Me_6, the expected initial product, $AlMe_2BHT$, is not observed. It was suggested that the disproportionation of $AlMe_2BHT$, shown in eq 3,

$$2AlMe_2BHT \rightleftharpoons {}^1/_2Al_2Me_6 + AlMeBHT_2 \quad (3)$$

is driven completely to the right by the enthalpy of formation of the trimethylaluminum dimer. We find this not to be the case. In fact, the reaction is more complex than that indicated even by eq 1. At room temperature, the NMR behavior is analogous to that observed in the Al_2Et_6 system. The terminal and bridging methyl groups of Al_2Me_6 are in fast exchange with the methyl groups of the mono-BHT species. The resonances of $AlMeBHT_2$ are observed separately. As the temperature is lowered, the complexity of the system begins to appear. At −80 °C, the bridging and terminal NMR resonances of Al_2Me_6 are clearly observed as are the resonances of $AlMeBHT_2$. The resonance attributable to the phenoxide portion of mono-BHT species is also observed, but the integrated intensity of the broad methyl resonance is unexpectedly large. At low ratios of phenoxide, the integration is for five methyl groups, and this integration decreases to two at high BHT ratios. This behavior is attributable to fast exchange between two species, Al_2Me_5BHT and $AlMe_2BHT$. The ratio of these two products is defined by the relative intensities of the phenoxide resonances and the methyl resonances. The data are satisfactorily modeled by the two concurrent disproportionations given in eq 4 and 5. The data and the fits calculated from the model

$$Al_2Me_5BHT \overset{K_4}{\rightleftharpoons} {}^1/_2Al_2Me_6 + AlMe_2BHT \quad (4)$$

$$3AlMe_2BHT \overset{K_5}{\rightleftharpoons} Al_2Me_5BHT + AlMeBHT_2 \quad (5)$$

are shown in Figure 3. The equilibrium constants at −80 °C are K_4 = 0.143 $M^{1/2}$ and K_5 = 55.5 M^{-1}.

In all of the NMR studies,there was never any evidence of $AlBHT_3$; all reactions stopped at $Al(R)BHT_2$. Though there is some confusion in the literature, this behavior is the same as that observed for reactions of H-BHT with $LiAlH_4$.[20] Both $AlMeBHT_2$ and $AlEtBHT_2$ react with added equivalents of *t*-BuOH indicating continued reactivity of the Al–R bonds. The only requirement is that the third ligand be smaller than the hindered H-BHT used in this study. Continued addition of *t*-BuOH leads to a complex mixture of alkoxides in which there is complete scrambling of the phenoxides and butoxides. Evolution of free H-BHT is observed in these mixtures.

Synthetic Studies. The NMR studies indicated that $AlEt_2BHT$ was a reasonable synthetic target. While the reaction goes to completion as expected, one obtains white crystalline material in a viscous liquid and a clean separation is not possible. The crystalline material is largely $AlEtBHT_2$, and the viscous liquid is a mixture of $AlEt_3$ and $AlEt_2BHT$. Unfortunately, $AlEtBHT_2$ seems to form a more stable crystalline phase than $AlEt_2BHT$ so that even from solutions where there is a high concentration of $AlEt_2BHT$, the predominant phase that crystallizes is $AlEtBHT_2$, shifting the disproportionation indicated in eq 3 to the right.

The bis-BHT species $Al(R)BHT_2$ are readily prepared and isolated as crystalline materials. We chose the simplest of these compounds, $AlMeBHT_2$, for a crystallographic investigation. The results of the structural de-

(20) (a) Haubenstock, H. *J. Org. Chem.* **1975**, *40*, 926. (b) Haubenstock, H.; Yang, N.-L. *J. Org. Chem.* **1978**, *43*, 1463. (c) Haubenstock, H.; Mester, T. A.; Zieger, H. *J. Org. Chem.* **1980**, *45*, 3443.

Table IV. Fractional Coordinates (×10⁴) and Isotropic Thermal Parameters for Non-Hydrogen Atoms in $AlMeBHT_2$

atom	*x*	*y*	*z*	*B*(iso), Å²
Al(1)	1048.8 (7)	1774.9 (7)	8098.1 (8)	1.8 (1)
O(1)	2097 (2)	2254 (2)	7911 (2)	2.0 (1)
O(2)	−209 (2)	2843 (2)	8348 (2)	2.0 (1)
C(1)	1155 (3)	203 (3)	7802 (3)	3.1 (1)
C(11)	3335 (2)	1908 (2)	7988 (2)	1.7 (1)
C(12)	3676 (2)	1721 (2)	6833 (2)	1.8 (1)
C(13)	4944 (2)	1352 (2)	6955 (3)	2.1 (1)
C(14)	5863 (2)	1192 (2)	8148 (3)	1.9 (1)
C(15)	5489 (2)	1434 (2)	9258 (3)	1.9 (1)
C(16)	4245 (2)	1795 (2)	9227 (3)	1.7 (1)
C(17)	2710 (3)	1935 (3)	5479 (3)	2.5 (1)
C(18)	3315 (3)	1838 (3)	4432 (3)	3.4 (1)
C(19)	2045 (3)	1046 (3)	5052 (3)	3.6 (1)
C(20)	1778 (3)	3143 (3)	5517 (3)	3.4 (1)
C(21)	3892 (2)	2143 (2)	10513 (3)	2.0 (1)
C(22)	5031 (3)	1751 (3)	11697 (3)	3.8 (1)
C(23)	2951 (3)	1619 (3)	10541 (3)	2.5 (1)
C(24)	3354 (3)	3431 (3)	10696 (3)	3.6 (1)
C(25)	7225 (2)	805 (2)	8221 (3)	2.4 (1)
C(31)	−1438 (2)	3173 (2)	8280 (2)	1.6 (1)
C(32)	−2366 (2)	3393 (2)	7061 (2)	1.8 (1)
C(33)	−3604 (2)	3723 (2)	7044 (3)	1.9 (1)
C(34)	−3962 (2)	3869 (2)	8141 (3)	1.9 (1)
C(35)	−3036 (2)	3679 (2)	9322 (3)	1.9 (1)
C(36)	−1771 (2)	3342 (2)	9438 (3)	1.8 (1)
C(37)	−2059 (3)	3331 (3)	5792 (3)	2.4 (1)
C(38)	−3230 (3)	3586 (4)	4616 (3)	4.7 (2)
C(39)	−1212 (3)	2167 (3)	5428 (3)	4.2 (1)
C(40)	−1448 (3)	4223 (3)	5955 (3)	4.0 (1)
C(41)	−803 (2)	3170 (2)	10790 (3)	2.3 (1)
C(42)	−1411 (3)	3495 (3)	11901 (3)	4.2 (1)
C(43)	−20 (3)	1912 (3)	10856 (3)	2.7 (1)
C(44)	16 (3)	3915 (3)	11094 (3)	2.8 (1)
C(45)	−5321 (2)	4263 (2)	8080 (3)	2.5 (1)

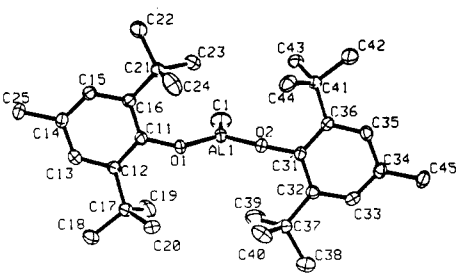

Figure 4. Perspective view of the molecule $AlMeBHT_2$ with atom labeling scheme. Thermal ellipsoids are drawn at the 40% level, and hydrogen atoms are omitted for clarity.

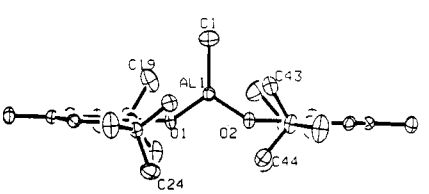

Figure 5. Alternative view of $AlMeBHT_2$ showing the unusual coplanarity of the two BHT groups.

Table V. Selected Bond Lengths (Å) and Bond Angles (deg) in $AlMeBHT_2$

Interatomic Distances			
Al(1)-O(1)	1.687 (2)	C(21)-C(23)	1.533 (4)
Al(1)-O(2)	1.685 (2)	C(21)-C(24)	1.526 (4)
Al(1)-C(1)	1.927 (3)	C(31)-C(32)	1.417 (3)
O(1)-C(11)	1.373 (3)	C(31)-C(36)	1.415 (3)
O(2)-C(31)	1.367 (3)	C(32)-C(33)	1.392 (3)
C(11)-C(12)	1.413 (3)	C(32)-C(37)	1.542 (4)
C(11)-C(16)	1.415 (3)	C(33)-C(34)	1.372 (4)
C(12)-C(13)	1.394 (4)	C(34)-C(35)	1.383 (4)
C(12)-C(17)	1.540 (4)	C(34)-C(45)	1.512 (3)
C(13)-C(14)	1.386 (4)	C(35)-C(36)	1.395 (3)
C(14)-C(15)	1.380 (4)	C(36)-C(41)	1.534 (3)
C(14)-C(25)	1.512 (3)	C(37)-C(38)	1.530 (4)
C(15)-C(16)	1.391 (3)	C(37)-C(39)	1.523 (4)
C(16)-C(21)	1.542 (3)	C(37)-C(40)	1.526 (4)
C(17)-C(18)	1.528 (4)	C(41)-C(42)	1.544 (4)
C(17)-C(19)	1.531 (4)	C(41)-C(43)	1.537 (4)
C(17)-C(20)	1.540 (4)	C(41)-C(44)	1.528 (4)
C(21)-C(22)	1.536 (4)		
Intramolecular Angles			
O(1)-Al(1)-O(2)	111.9 (1)	C(16)-C(21)-C(24)	108.6 (2)
O(1)-Al(1)-C(1)	123.9 (1)	C(22)-C(21)-C(23)	105.5 (2)
O(2)-Al(1)-C(1)	123.6 (1)	C(22)-C(21)-C(24)	108.5 (3)
Al(1)-O(1)-C(11)	140.5 (2)	C(23)-C(21)-C(24)	109.6 (2)
Al(1)-O(2)-C(31)	146.8 (2)	C(32)-C(31)-C(36)	120.7 (2)
O(1)-C(11)-C(12)	119.4 (2)	C(31)-C(32)-C(33)	117.4 (2)
O(1)-C(11)-C(16)	119.5 (2)	C(31)-C(32)-C(37)	122.8 (2)
O(2)-C(31)-C(32)	119.7 (2)	C(33)-C(32)-C(37)	119.7 (2)
O(2)-C(31)-C(36)	119.5 (2)	C(32)-C(33)-C(34)	123.5 (2)
C(12)-C(11)-C(16)	121.1 (2)	C(33)-C(34)-C(35)	117.8 (2)
C(11)-C(12)-C(13)	117.4 (2)	C(33)-C(34)-C(45)	121.6 (2)
C(11)-C(12)-C(17)	122.7 (2)	C(35)-C(34)-C(45)	120.6 (2)
C(13)-C(12)-C(17)	119.8 (2)	C(34)-C(35)-C(36)	123.0 (2)
C(12)-C(13)-C(14)	123.0 (2)	C(31)-C(36)-C(35)	117.6 (2)
C(13)-C(14)-C(15)	117.7 (2)	C(31)-C(36)-C(41)	122.7 (2)
C(13)-C(14)-C(25)	120.6 (2)	C(35)-C(36)-C(41)	119.7 (2)
C(15)-C(14)-C(25)	121.6 (2)	C(32)-C(37)-C(38)	112.0 (2)
C(14)-C(15)-C(16)	123.2 (2)	C(32)-C(37)-C(39)	112.9 (2)
C(11)-C(16)-C(15)	117.5 (2)	C(32)-C(37)-C(40)	108.9 (2)
C(11)-C(16)-C(21)	122.2 (2)	C(38)-C(37)-C(39)	105.9 (3)
C(15)-C(16)-C(21)	120.2 (2)	C(38)-C(37)-C(40)	107.1 (3)
C(12)-C(17)-C(18)	122.1 (2)	C(39)-C(37)-C(40)	109.9 (3)
C(12)-C(17)-C(19)	109.5 (2)	C(36)-C(41)-C(42)	112.5 (2)
C(12)-C(17)-C(20)	110.3 (2)	C(36)-C(41)-C(43)	109.7 (2)
C(18)-C(17)-C(19)	107.0 (2)	C(36)-C(41)-C(44)	110.8 (2)
C(18)-C(17)-C(20)	106.5 (2)	C(42)-C(41)-C(43)	106.0 (2)
C(19)-C(17)-C(20)	111.3 (2)	C(42)-C(41)-C(44)	106.2 (2)
C(16)-C(21)-C(22)	111.6 (2)	C(43)-C(41)-C(44)	111.5 (2)
C(16)-C(21)-C(23)	113.0 (2)		

termination are given in Table IV with the important bond distances and angles given in Table V. The structure is depicted in Figures 4 and 5; the atom-labeling scheme is given Figure 4, and an alternative view of the structure is given in Figure 5. The structure consists of discrete, monomeric units with a three-coordinate aluminum center.[21] The molecule adopts an interesting structure in which the two BHT rings are almost coplanar. This is graphically demonstrated in the alternate view of the molecule. The aluminum atom and its pendant methyl group are on a vector almost perpendicular to the plane defined by the two BHT rings. Another description would be that the plane defined by the C, Al, O_2 group is perpendicular to the planes defined by the two BHT groups (91.3 and 88.1°). The six-electron aluminum is 0.08 Å out of the plane defined by O–O–C. Interestingly, this slight distortion is toward hydrogen atom (H23″) of a methyl of the *tert*-butyl group of the BHT, yielding an Al–H distance of 1.95 Å. Bonding interactions of electron-deficient, early d-block, lanthanide, and actinide metals with hydrocarbon

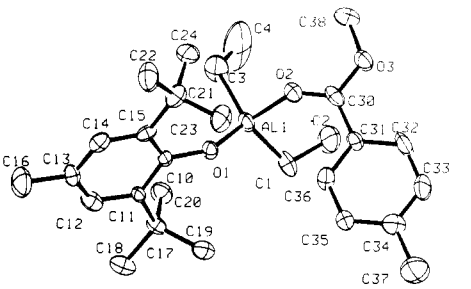

Figure 6. Perspective view of the molecule $AlEt_2BHT$-($MeO_2CC_6H_4CH_3$) showing the atom labeling scheme. Thermal ellipsoids are drawn at the 40% level and hydrogen atoms are omitted for clarity.

fragments of coordinated ligands has been noted.[22] This interaction could indicate that the same type of weak bonding can occur in electron-deficient main-group species. The corresponding distance on the opposite side is 2.28 Å for Al–H39″. The two BHT groups are bulkier than the methyl group, but the O–Al–O angle is only 111.9° while the two O–Al–C angles are 123.6 and 123.9°. The Al–O–C angles of 140.5 and 146.8° minimize the contacts between the *tert*-butyl groups of the BHT ligands. These angles are centered in the wide range of M–O–C angles observed in other structures; they are small compared to angles observed in transition-metal complexes where π-interactions become important[23] but large compared with other main-group structures.[24,25] The Al–O distances are short compared to the normally accepted range of 1.8–2.0 Å.[26] The observed Al–C distance is within the range normally observed in the solid state but is short in comparison with the distances for other monomeric, three-coordinate species such as gas phase $AlMe_3$.[27]

Reactions with Aromatic Esters. We were also very interested in the combined role of BHT and aromatic esters in our nonclassical catalysts so we began to investigate the sequential reaction of H-BHT and methyl toluate with triethylaluminum. NMR scale reactions indicate formation of a complex between $AlEt_2BHT$ and methyl toluate. The *tert*-butyl groups of the BHT shift from 1.45 to 1.61 ppm, and the resonances of the coordinated methyl toluate were significantly different from those of free methyl toluate. The ethyl groups of the aluminum alkyl were shifted downfield. Infrared spectroscopy indicated a shift in the ester C=O from 1725 cm^{-1} for free ligand to 1635 cm^{-1} upon complexation. The reaction of triethylaluminum to give complexed species and then to alkylate the C=O bond to give aluminum alkoxides has been reported.[28] We see no evidence of further reaction after initial adduct formation even after long periods of time or upon heating. The diminished reducing power of the phenoxide-modified aluminum alkyls seems to preclude this reaction.

(21) Jerius, J. J.; Hahn, J. M.; Rahman, A. F. M. M.; Mols, O.; Ilsley, W. H.; Oliver, J. P. *Organometallics* **1986**, *5*, 1812.

(22) (a) Fanwick, P. E.; Ogilvy, A. E.; Rothwell, I. P. *Organometallics* **1987**, *6*, 73 and references therein. (b) Brookhart, M.; Green, M. L. H. *J. Organomet. Chem.* **1983**, *250*, 395 and references therein.

(23) (a) Chamberlain, L. R.; Rothwell, I. P.; Huffman, J. C. *Inorg. Chem.* **1984**, *23*, 2575. (b) Latesky, S. L.; Keddington, J.; McMullen, A. K.; Rothwell, I. P.; Huffman, J. C. *Inorg. Chem.* **1985**, *24*, 995.

(24) Geerts, R. L.; Huffman, J. C.; Caulton, K. G. *Inorg. Chem.* **1986**, *25*, 1803.

(25) Calabrese, J.; Cushing, M. A.; Ittel, S. D. *Inorg. Chem.*, accepted for publication.

(26) (a) Zaworotko, M. J.; Rogers, R. D.; Atwood, J. L. *Organometallics* **1982**, *1*, 1179. (b) Atwood, J. L.; Zaworotko, M. J. *J. Chem. Soc., Chem. Commun.* **1983**, 302.

(27) Almenningen, A.; Halvorsen, S.; Haaland, A. *Acta Chem. Scand.* **1971**, *25*, 1937.

(28) (a) Chien, J. C. W.; Wu, J.-C. *J. Polym. Sci., Polym. Chem. Ed.* **1982**, *20*, 2445. (b) Busico, V.; Corradini, P.; De Martino, L.; Proto, A.; Savino, V. *Makromol. Chem.* **1985**, *186*, 1279.

Table VI. Fractional Coordinates (×10⁴) and Isotropic Thermal Parameters for Non-Hydrogen Atoms in $AlEt_2BHT(MeO_2CC_6H_4Me)$

atom	*x*	*y*	*z*	*B*(iso), Å²
Al(1)	1708 (1)	3277 (2)	3048 (2)	2.5 (1)
O(1)	1276 (2)	2519 (3)	2505 (3)	1.9 (2)
O(2)	1899 (2)	4054 (4)	2125 (4)	3.0 (2)
O(3)	2203 (2)	5352 (4)	1615 (4)	3.2 (2)
C(1)	1366 (3)	4138 (5)	3849 (5)	3.1 (3)
C(2)	1702 (4)	4970 (6)	4090 (7)	4.8 (3)
C(3)	2406 (3)	2770 (6)	3441 (6)	4.7 (3)
C(4)	2769 (5)	3232 (8)	3940 (11)	13.8 (7)
C(10)	1150 (3)	1640 (5)	2377 (5)	1.8 (2)
C(11)	829 (3)	1193 (5)	3002 (5)	1.8 (2)
C(12)	721 (3)	285 (6)	2870 (5)	2.7 (3)
C(13)	891 (3)	−178 (5)	2144 (6)	2.4 (2)
C(14)	1173 (3)	287 (6)	1518 (6)	2.4 (3)
C(15)	1305 (3)	1198 (6)	1607 (5)	2.0 (2)
C(16)	776 (4)	−1159 (6)	2018 (6)	4.6 (3)
C(17)	618 (3)	1632 (5)	3850 (5)	2.1 (2)
C(18)	230 (3)	1033 (6)	4361 (5)	3.3 (3)
C(19)	301 (3)	2497 (6)	3656 (5)	3.0 (3)
C(20)	1112 (3)	1813 (6)	4474 (5)	3.0 (3)
C(21)	1617 (3)	1675 (6)	862 (6)	3.2 (3)
C(22)	1697 (4)	1068 (6)	63 (6)	4.4 (3)
C(23)	1299 (3)	2494 (6)	529 (5)	3.6 (3)
C(24)	2181 (3)	1962 (5)	1200 (6)	3.5 (3)
C(30)	1809 (3)	4812 (6)	1811 (5)	2.5 (3)
C(31)	1254 (3)	5170 (5)	1627 (6)	2.3 (2)
C(32)	1187 (4)	6079 (6)	1441 (6)	3.6 (3)
C(33)	663 (4)	6404 (5)	1292 (6)	3.9 (3)
C(34)	219 (3)	5846 (6)	1289 (5)	3.0 (3)
C(35)	293 (3)	4938 (5)	1471 (6)	3.1 (3)
C(36)	811 (3)	4609 (5)	1647 (5)	2.8 (3)
C(37)	−347 (4)	6215 (7)	1119 (7)	5.5 (4)
C(38)	2759 (3)	5068 (6)	1830 (6)	3.8 (3)

The crystal structure of $AlEt_2BHT$·(methyl toluate) was determined as a model for the interaction of aromatic esters with aluminum alkyls in the active polymerization catalysts. Results of the determination are given in Table VI, and important bond distances and angles are given in Table VII. A perspective view of the molecule with the atom-labeling scheme is given in Figure 6.

The structure consists of discrete, monomeric units. Geometry about the aluminum atom is approximately tetrahedral. Of the six angles about the aluminum atom, the three largest are associated with the covalent bonds to the ethyl groups and the phenoxide. The three angles associated with the aluminum to carbonyl oxygen atom are all relatively acute. These features indicate that the structure about aluminum retains some of its original three-coordinate, planar character with the carbonyl oxygen providing the distortion to tetrahedral. In agreement with expected trends for sp^3 versus sp^2 for first-row elements, the Al–X bond distances observed in this structure are longer than those observed in the three-coordinate structure above and correspond more closely to previously observed structures. The Al–O–C angle of the phenoxide is once again opened up to 145.6°, consistent with the structure above. The distance between the aluminum and the carbonyl oxygen is considerably longer than that observed for the Al–O bond to the phenoxide, again consistent with the view that the carbonyl coordination is a secondary effect in the bonding about aluminum. The Al–O–C angle to the carbonyl of 143.0° and the torsion angle about the carbonyl C–O bond (O3–C3O–O2–Al) of 130.1° place the aluminum atom in a region of moderate C=O lone-pair electron density as determined by studies involving hydrogen bonding to carbonyls.[29] A higher torsion angle about the C=O bond would result in better lone-pair overlap but would also increase steric interactions with the phenyl group of the benzoate ligand.

Table VII. Selected Bond Lengths (Å) and Bond Angles (deg) in $AlEt_2BHT(MeO_2CC_6H_4Me)$

Interatomic Distances			
Al(1)–O(1)	1.749 (5)	C(14)–C(15)	1.404 (10)
Al(1)–O(2)	1.887 (6)	C(15)–C(21)	1.552 (11)
Al(1)–C(1)	1.970 (9)	C(17)–C(18)	1.528 (10)
Al(1)–C(3)	1.958 (9)	C(17)–C(19)	1.532 (10)
O(1)–C(10)	1.360 (8)	C(17)–C(20)	1.552 (10)
O(2)–C(30)	1.246 (9)	C(21)–C(22)	1.532 (11)
O(3)–C(30)	1.297 (8)	C(21)–C(23)	1.530 (10)
O(3)–C(38)	1.461 (9)	C(21)–C(24)	1.531 (11)
C(1)–C(2)	1.532 (10)	C(30)–C(31)	1.486 (10)
C(3)–C(4)	1.349 (13)	C(31)–C(32)	1.395 (10)
C(10)–C(11)	1.414 (10)	C(31)–C(36)	1.374 (10)
C(10)–C(15)	1.402 (10)	C(32)–C(33)	1.390 (11)
C(11)–C(12)	1.395 (10)	C(33)–C(34)	1.370 (11)
C(11)–C(17)	1.546 (10)	C(34)–C(35)	1.394 (10)
C(12)–C(13)	1.373 (10)	C(34)–C(37)	1.513 (11)
C(13)–C(14)	1.375 (10)	C(35)–C(36)	1.386 (10)
C(13)–C(16)	1.504 (10)		
Intramolecular Angles			
O(1)–Al(1)–O(2)	101.7 (3)	C(10)–C(15)–C(14)	118.1 (8)
O(1)–Al(1)–C(1)	116.9 (3)	C(10)–C(15)–C(21)	122.6 (7)
O(1)–Al(1)–C(3)	114.6 (3)	C(14)–C(15)–C(21)	119.3 (8)
O(2)–Al(1)–C(1)	100.0 (3)	C(11)–C(17)–C(18)	113.5 (7)
O(2)–Al(1)–C(3)	103.7 (3)	C(11)–C(17)–C(19)	111.9 (6)
C(1)–Al(1)–C(3)	116.4 (4)	C(11)–C(17)–C(20)	108.3 (6)
Al(1)–O(1)–C(10)	145.6 (5)	C(18)–C(17)–C(19)	105.8 (6)
Al(1)–O(2)–C(30)	143.0 (6)	C(18)–C(17)–C(20)	106.1 (6)
C(30)–O(3)–C(38)	117.8 (7)	C(19)–C(17)–C(20)	111.1 (6)
Al(1)–C(1)–C(2)	116.3 (6)	C(15)–C(21)–C(22)	112.4 (7)
Al(1)–C(3)–C(4)	122.7 (8)	C(15)–C(21)–C(23)	110.7 (7)
O(2)–C(30)–O(3)	121.6 (8)	C(15)–C(21)–C(24)	109.8 (7)
O(1)–C(10)–C(11)	119.1 (8)	C(22)–C(21)–C(23)	106.3 (7)
O(1)–C(10)–C(15)	120.6 (7)	C(22)–C(21)–C(24)	107.6 (7)
O(2)–C(30)–C(31)	123.7 (7)	C(23)–C(21)–C(24)	109.9 (7)
O(3)–C(30)–C(31)	114.7 (8)	C(30)–C(31)–C(32)	119.5 (8)
C(11)–C(10)–C(15)	120.1 (7)	C(30)–C(31)–C(36)	120.1 (7)
C(10)–C(11)–C(12)	118.0 (8)	C(32)–C(31)–C(36)	120.5 (8)
C(10)–C(11)–C(17)	124.1 (7)	C(31)–C(32)–C(33)	118.5 (8)
C(12)–C(11)–C(17)	117.8 (8)	C(32)–C(33)–C(34)	121.5 (8)
C(11)–C(12)–C(13)	123.0 (8)	C(33)–C(34)–C(35)	119.4 (8)
C(12)–C(13)–C(14)	117.9 (8)	C(33)–C(34)–C(37)	120.5 (9)
C(12)–C(13)–C(16)	122.2 (9)	C(35)–C(34)–C(37)	120.2 (8)
C(14)–C(13)–C(16)	119.9 (9)	C(34)–C(35)–C(36)	119.8 (8)
C(13)–C(14)–C(15)	122.6 (8)	C(31)–C(36)–C(35)	120.3 (8)

Discussion

On the basis of simple phenoxide,[30] one would expect to observe a stable, oxygen-bridged dimer, $Al_2Me_4BHT_2$, but such is not the case. Though it was not possible to freeze out the NMR spectrum of Al_2Me_5BHT to confirm the mode of bridging, it is likely that it is bridged through two methyl groups as in Al_2Me_6 rather then one methyl and one phenoxide. In such a structure the steric interactions of the BHT *tert*-butyl groups would be limited to one tetrahedral aluminum center rather that the two if the BHT were bridging. In the structure of the tetrahedral methyl toluate complex, both ethyl groups are turned away from the BHT ligand to minimize steric congestion.

For BHT exchange between aluminum centers to take place, the aluminum atoms must be oxygen bridged at least as a transition state. Our structure of the methyl toluate adduct demonstrates four-coordinate aluminum in a mono-BHT system, but it is increasingly difficult to achieve four-coordination as the number of BHT groups is increased. In the dimeric species $[MgBHT_2]_2$, three

(29) Murray-Rust, P.; Glusker, J. P. *J. Am. Chem. Soc.* **1984**, *106*, 1018.

(30) Starowieyski, K.; Pasynkiewicz, S.; Skowronska, M. D. *J. Organomet. Chem.* **1971**, *31*, 149.

BHT groups are coordinated to each magnesium atom,[25] but the ionic radius of magnesium is 0.2 Å larger than aluminum. In the aluminum system, disproportionation of two $Al(R)BHT_2$ or H-BHT attack on $Al(R)BHT_2$ to give $AlBHT_3$ would require not three, but four-coordination with three BHT groups on a single center. Clearly, this is not a favored structure, even as a transition state along a reaction coordinate.

In the activation of heterogeneous Ziegler–Natta catalysts, the observed steric crowding is going to play a major role. The BHT-substituted aluminum alkyl will be restricted in its approach to the $TiCl_4$ or $TiCl_3$ surface species so only the most accessible will be able to react. The diminished reducing power of the BHT-substituted aluminum alkyls, reflected in their reaction with the ester Lewis bases, is also going to be a factor in their reactivity with titanium species on the catalyst. The catalyst is less likely to be overreduced to inactive $TiCl_2$ species.[31]

Conclusions about increased steric constraints and diminished reducing power are complicated by the observed disproportionation of the mono-BHT species. The less sterically hindered and more strongly reducing AlR_3 species will always be present unless 2 equiv of BHT are used. The observation that only 1 equiv of BHT is required in the aluminum alkyl activator indicates that the incorporation of H-BHT into the titanium center during the preparation of $MgCl_2$-supported catalysts apparently protects the active Ti centers from unwanted reduction by the Al_2Et_6 formed by disproportionation. Thus, $AlEt_2BHT$ is still capable of eliciting the observed[17] nonclassical behavior despite the disproportionation reactions observed here.

(31) Goodall, B. L. *J. Chem. Educ.* **1986**, *63*, 191.

Acknowledgment. We wish to acknowledge the skilled technical assistance of Martin A. Cushing, Jr., Lou Lardeer, Elwood Conaway, and Wayne King. Discussion of the thermodynamic measurements with Patricia L. Watson were particularly helpful.

Registry No. H-BHT, 128-37-0; $AlEtBHT_2$, 61986-88-7; $AlEt_2BHT$, 61986-89-8; $AlMeBHT_2$, 56252-55-2; $Al(i\text{-}Bu)BHT_2$, 56252-57-4; $AlEt_2BHT(MT)$, 111847-26-8; MT, 25567-11-7; $AlEt_3O$, 97-93-8; *t*-BuOH, 75-65-0; $AlMe_3$, 75-24-1; $Al(i\text{-}Bu)_3$, 100-99-2.

Supplementary Material Available: Data used for determination of equilibrium constants, plots of equilibrium constants as a function of BHT to aluminum ratios, and listings of anisotropic thermal parameters, hydrogen atom parameters, and additional bond distances and angles (13 pages); tables of calculated and observed structure factors (14 pages). Ordering information is given on any current masthead page.

Synthesis and Reactivity of Ditungsten μ-Carbene Complexes: X-ray Crystal Structure of $W_2(CO)_9[\mu\text{-}\eta^1,\eta^3\text{-}C(OCH_3)\overline{C{=}CH(CH_2)_5CH_2}]$

David W. Macomber* and Mong Liang

Department of Chemistry, Kansas State University, Manhattan, Kansas 66506

Robin D. Rogers*

Department of Chemistry, Northern Illinois University, DeKalb, Illinois 60115

Received June 22, 1987

A series of ditungsten complexes, $W_2(CO)_9[\mu\text{-}\eta^1,\eta^3\text{-}C(OCH_3)C(R^1){=}CHR^2]$ (**3**), containing $\mu\text{-}\eta^1,\eta^3$-allylidene ligands have been prepared in moderate to excellent yields from Fischer-type α,β-unsaturated tungsten carbene complexes, $(CO)_5W[C(OCH_3)C(R^1){=}CHR^2]$ (**1**) and $(CO)_5W{\cdot}THF$ (**2**). These complexes (**3**) were purified on silica gel at −20 to −30 °C followed by crystallization to produce, in most cases, dark red crystalline materials. All new compounds were characterized by elemental analyses and ^1H and ^{13}C NMR spectroscopy. When $W_2(CO)_9[\eta^1,\eta^3\text{-}C(OCH_3)\overline{C{=}CH(CH_2)_2CH_2}]$ (**3d**) was treated with CO in C_6D_6 solution, it was cleanly converted to the cyclopentenyl Fischer–carbene complex $(CO)_5W[C(OCH_3)\overline{C{=}CH(CH_2)_2CH_2}]$ (**1d**) and $W(CO)_6$. $W_2(CO)_9[\mu\text{-}\eta^1,\eta^3\text{-}C(OCH_3)\overline{C{=}CH(CH_2)_5CH_2}]$ (**3f**), which contains a cyclooctene ring as part of the $\mu\text{-}\eta^1,\eta^3$-allylidene ligand, was further characterized by variable-temperature ^{13}C NMR spectroscopy and single-crystal X-ray diffraction methods. Complex **3f** crystallizes in the monoclinic space group $P2_1/c$ with (at −150 °C) a = 9.832 (4) Å, b = 10.424 (3) Å, c = 21.120 (6) Å, β = 93.37 (3)°, and D_{calcd} = 2.37 g cm^{-3} for Z = 4. Least-squares refinement based on 3394 independent observed [$F_o \geq 5\sigma(F_o)$] reflections led to a final conventional R value of 0.038.

Introduction

Over the past fifteen years there have been numerous reports concerning the preparation, reactivity, and structures of dimetallic complexes containing $\mu\text{-}\eta^1,\eta^3$-allylidene ligands. Represented in Chart I are the four possible extreme bonding modes (A–D) for such complexes. For most of the reported complexes, M(1) and M(2) are the same, which include derivatives of molybdenum,[1] tungsten,[2]

0276-7333/88/2307-0416$01.50/0